Available online at www.sciencedirect.com
SCIENCE DIRECT
ELSEVIER
Palaeogeography, Palaeoclimatology, Palaeoecology 232 (2006) 36–52
PALAEO
www.elsevier.com/locate/palaeo

Paleoceanographic history around the Tsugaru Strait between the Japan Sea and the Northwest Pacific Ocean since 30 cal kyr BP

Itaru Koizumi [a,*], Ryuji Tada [b], Hisashi Narita [c], Tomohisa Irino [d], Takafumi Aramaki [e], Tadamichi Oba [f], Hirofumi Yamamoto [g]

[a] *Atsubetsu-kita 3-5-18-2, Atsubetsu-ku, Sapporo 004-0073, Japan*
[b] *Graduate School of Science, University of Tokyo, Tokyo, Japan*
[c] *Department of Oceanography, Tokai University, Shimizu, Japan*
[d] *Graduate School of Environmental Earth Science, Hokkaido University, Japan*
[e] *Marine Research Laboratory, Japan Atomic Energy Research Institute, Mutsu, Japan*
[f] *Sendagaya 2-2-3, Shibuya-ku, Tokyo 115-0051, Japan*
[g] *Japan Agency for Marine-Earth Science and Technology, Yokosuka, Japan*

Received 25 February 2005; received in revised form 13 July 2005; accepted 5 September 2005

Abstract

The paleoceanographic history around the Tsugaru Strait since 30.0 cal kyr BP was reconstructed using ecological and biogeographical habitats of diatom species and Q-mode factor analysis of diatom flora in six piston cores. At 30.0–17.5 cal kyr BP, a fall in sea level and the intensification of the Oyashio Current caused erosion of submarine sediments near the shore in the eastern area of the Strait and led to deposition of the third and second sequences of thinly laminated layers (TL3 and TL2) in the Japan Sea. At 17.5–11.5 cal kyr BP, cooling intensified around the Strait, producing an inflow of Oyashio water into the Japan Sea through the Strait. At 15.5–14.5 cal kyr BP, a cold-water mass around the Strait developed from subarctic sea-ice to arctic waters. At 13.0–11.2 cal kyr BP, the Younger Dryas cooling was clearly recorded by the increasing of oceanic cold-water diatom species in the eastern area of the Tsugaru Strait but not in the Japan Sea. At 15.5–13.0 cal kyr BP and 11.25–10.25 cal kyr BP, the warming around the Younger Dryas resulted in the deposition of thinly laminated layers off Shimokita in the eastern area of the Strait. At 9.5 cal kyr BP, the Oyashio Current water intruded into deep depths in the mixed water region off Sanriku. At 9.5–7.0 cal kyr BP, the fluctuation of 1.5-kyr intervals in the strength of the Tsushima Warm Current system in the Japan Sea was initiated.

Keywords: Japan Sea; Diatoms; MD01-2409; Tsushima Warm Current; Tsugaru Warm Current; Oyashio Current; Thinly laminated layer; Younger Dryas cooling

1. Introduction

The Japan Sea is a marginal sea, connecting to the Northwest Pacific Ocean and to adjoining marginal seas by the narrow and shallow Tsushima (Korea) (sill depth 130 m), Tsugaru (130 m), Soya (55 m), and Mamiya (Tartar) (15 m) straits. The Tsushima Warm Current (TWC) flows into the Japan Sea from the East China Sea through the Tsushima Strait between Kyushu and Korea. The TWC flows along the western margin of Honshu Island and most of the TWC flows out to the Pacific Ocean through the Tsugaru Strait

* Corresponding author.
E-mail address: itaru@sci.hokudai.ac.jp (I. Koizumi).

0031-0182/$ - see front matter © 2005 Elsevier B.V. All rights reserved.
doi:10.1016/j.palaeo.2005.09.003

between Honshu and Hokkaido. The TWC flows above the Japan Sea Proper Water (JSPW), which is a homogeneous cold water-mass deeper than 200–300 m that forms in the northwestern part of the Japan Sea by the subsidence of strongly cooled surface water (Fig. 1).

The TWC converges southwest of the Tsugaru Strait and then diverges into two branches in western area of the Strait. One branch is Tsugaru Warm Current, which flows into the Northwest Pacific Ocean through the Tsugaru Strait. The other flows along the west coast of the Hokkaido Island as the Northward Current (Onishi and Ohtani, 1997), and flows out to the Okhotsk Sea through the Soya Strait between Hokkaido and Sakhalin. Ohtani and Nishida (1990) reported that the total transport of the modern Tsugaru Warm Current near shore was extremely variable 1–31% of the TWC. However, the TWC deeper than 500 m on the west side of the Tsugaru Strait splits into half, the Northward Current and the Tsugaru Warm Current, with equal average volumes of transport (Onishi and Ohtani, 1997).

Along the southeast coast of Hokkaido, the Oyashio Current flows southward down to approximately Lat. 41°N. The Tsugaru Warm Current flows southward to approximately Lat. 38°N off Kinkazan Island and occasionally comes in contact with the Oyashio Intrusion which forms a tongue-like shape ~160 km in width (Kawai, 1972). The Oyashio Intrusion water subsides as North Pacific Intermediate Water, which is characterized with a salinity minimum (Yasuda et al., 1996).

The Japan Sea responded distinctly to sea level fluctuations during the last glacial–interglacial period. Oba et al. (1991) presented four distinct stages of environmental changes which were modified chronologically by Oba et al. (1995): (1) the surface water was freshened and distinctly stratified from 30–14 ^{14}C kyr BP and salinity reached a minimum at 15 ^{14}C kyr BP, (2) the Oyashio Current entered into the Japan Sea from 14–10 ^{14}C kyr BP, (3) TWC temporally formed from 10–8 ^{14}C kyr BP, and (4) the modern oceanographic regime was established after 8 ^{14}C kyr BP.

Tada et al. (1999) noted that the strong penetration of waters from the East China Sea into the Japan Sea

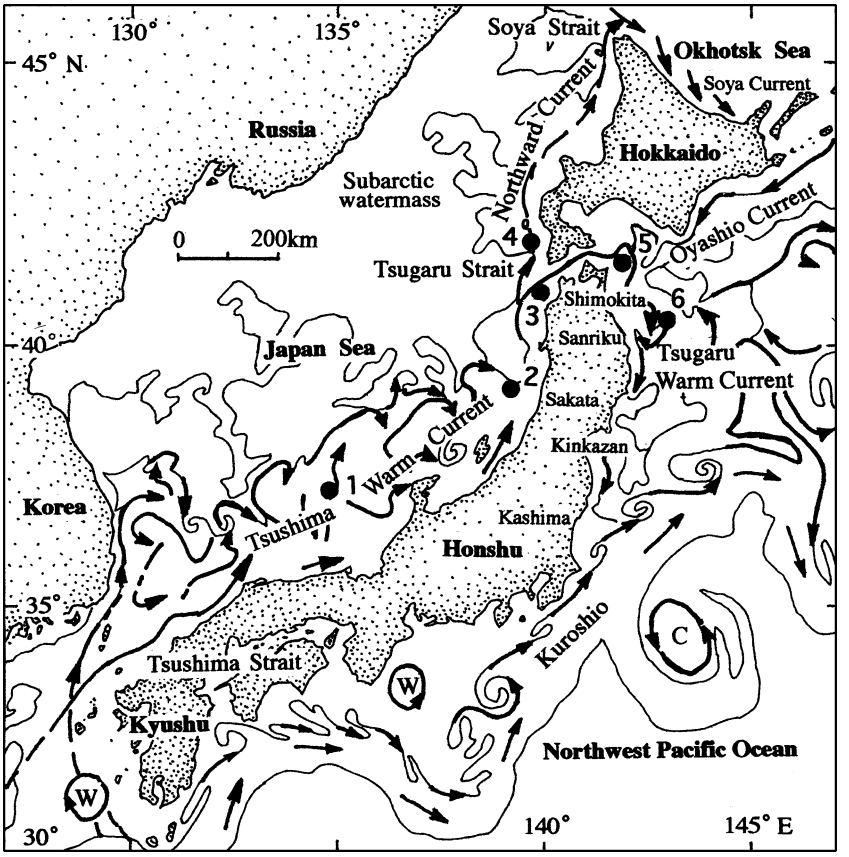

Fig. 1. Location (black circles) of six cores. 1=D-GC-6, 2=KH-86-2-9, 3=KH-84-3-33, 4=KH-84-3-9, 5=MD01-2409, 6=MR97-04-1. Arrows indicate flow of the currents and contour interval show the boundary between water masses. W=warm-water, C=cold-water.

Table 1
Cores studied in this paper

Area	No.	Core	Lat. (°N)	Long. (°E)	Depth (m)	Core length (cm)	Area
Japan Sea	1	D-GC-6	37.07	134.70	946	270	Ridge
	2	KH-86-2-9	39.31	139.03	760	770	Continental slope
	3	KH-84-3-33	40.92	139.87	835	674	Continental slope
	4	KH-84-3-9	41.83	139.16	2280	735	Ridge
Tsugaru Strait							
Northwest Pacific	5	MD01-2409	41.56	141.87	975	4467	Continental slope
	6	MR97-04-1	40.56	142.93	1520	20+683	Submarine hill

reduced deep water ventilation and enhanced the surface productivity, leading to the development of anoxic bottom water conditions and deposition of the laminated dark layers, which seem to be corresponding to an interstadial.

The mechanism of the Oyashio intrusion into the Japan Sea through the Tsugaru Strait 14–10 ^{14}C kyr BP was explained using a box model of baroclinic transport by Ikeda et al. (1999). Takei et al. (2002) corroborated this model using data from two piston cores taken oceanographically from west of the Tsugaru Strait, concluding that the Oyashio Current continued to flow into the Japan Sea through the Tsugaru Strait driven by baroclinic transport, and coexisted with the TWC in the Japan Sea between 8.3 and 4.8 cal kyr BP.

Although the Holocene can be described as being comparatively stable, the TWC oscillated in strength at ~1.5-kyr intervals. These oscillations can be correlated with worldwide climatic fluctuations since the Holocene deglaciation (Koizumi, 1989; Bond et al., 1999; Takei et al., 2002; Shimada et al., 2004).

In this paper we investigate the paleoceanography using diatom floras from core sediments at both the Japan Sea and the Northwest Pacific sides of the Tsugaru Strait, and investigate the cause of formation of thinly laminated layers that are recognized in cores during the latest Quaternary.

2. Core materials and sediment age model

Gravity core D-GC-6 (Table 1, Fig. 1), which was taken atop Oki Ridge at 946 m water depth, is composed of alternating layers of homogeneous light olive colored silty clay and laminated or bioturbated dark colored silty clay. Thin laminated clay is intercalated at 245.5–233.5 cm, corresponding to TL3, 226.5–199.5 cm to TL2, and 154.3–155.0 cm to TL1, and Aira-Tanzawa (AT) tephra at 273.5–263.3 cm, and Kikai-Akahoya (K-Ah) tephra at 118cm (Koizumi and Tada, per. comm.).

An age mode for core D-GC-6 was constructed on the basis of many AMS ^{14}C assigned by Yokoyama et al. (per. comm.) (Table 2).

Piston core KH-86-2-9 was recovered from beneath the main track of the TWC off Sakata and is composed of olive gray colored homogeneous clay with intercalated thin laminated clay at between 605–593 cm, corresponding to TL4, 584–576 cm to TL3, 570–490 cm to TL2, and 377–370 cm to TL1, and AT tephra at 633–630 cm.

Two piston cores each, recovered on either side of the Tsugaru Strait, KH-84-3-33 and KH-84-3-9 in the Japan Sea, and MD01-2409 and MR97-04-1 in the Northwest Pacific Ocean, were also used in this study.

KH-84-3-33 is composed of olive gray colored homogeneous mud with an intercalated thin ash layer Baegdusan-Tomakomai (B-Tm) at 32.5–31.0 cm, corresponding to ~0.7 cal kyr BP (Machida and Arai, 1992).

KH-84-3-9 is composed of grayish olive colored clay with intercalated mottled clay and a high abundance of foraminiferal tests at 182–175 cm, corresponding to 12.1–11.5 cal kyr BP. Laminated clay occurs at 175–173 cm correlated to TL1, fine grained sand occurs at 70–68 cm (3.9–3.8 cal kyr BP) and 58–53 cm (3.2–2.9 cal kyr BP), and the Baegdusan-Tomakomai Ash layer occurs at 23.8–20.6 cm (~1 cal kyr BP).

The age model for the four cores taken from the Japan Sea is shown in Table 3. The peaks of the diatom species *Fragilariopsis doliolus* in such three cores as KH-86-2-9, KH-84-3-33, and KH-84-3-9 were corre-

Table 2
Chronostratigraphic framework (depth vs. calendar age) in D-GC-6

Depth (cm)	Cal kyr BP	Methods
20.62	0.79	AMS^{14}C
118.00	7.20	K-Ah tephra
151.32	11.10	AMS^{14}C
168.82	13.34	AMS^{14}C
201.32	18.75	AMS^{14}C
225.12	23.53	AMS^{14}C
243.82	27.67	AMS^{14}C
263.30	29.71	Top of AT tephra

Table 3
Chronostratigraphic framework (depth vs. calendar age) in D-GC-6, KH-86-2-9, KH-84-3-33, KH-84-3-9, and MR97-4-1

Events	Depth (cm)	D-GC-6	KH-86-2-9	KH-84-3-33	KH-84-3-9	MR97-4-1
		Cal kyr BP	Depth (cm)	Depth (cm)	Depth (cm)	Depth (cm)
Peak of *F. doliolus*	12.77	0.49		10.0		
Peak of *F. doliolus*	15.21	0.58	5.0	20.0	5.0	
Peak of *F. doliolus*	23.72	0.99			20.0	
Peak of *F. doliolus*	42.55	2.23	75.0	160.0		
Peak of *F. doliolus*	51.51	2.82				
Peak of *F. doliolus*	58.90	3.31	105.0	220.0	60.0	(Gravity) 8.0
Peak of *F. doliolus*	83.52	4.93	175.0	400.0	85.0	17.5
Peak of *F. doliolus*	103.22	6.23	235.0	560.0	105.0	
Peak of *F. doliolus*	105.68	6.39		590.0	115.0	(Piston) 1.0
Peak of *F. doliolus*	109.38	6.63	275.0	620.0		4.0
Peak of *F. doliolus*	126.62	8.21				
Base of TL1/D1	154.30	11.4	377.0		175.0	
Top of TL2/D2	199.00	17.00	449.0		234.0	
Base of TL3/D3	246.00	27.90	584.0			
Top of AT	263.30	29.71	630.0			

lated with those in the core D-GC-6, for which the age model was constructed on the basis of many AMS ^{14}C dates (Table 2). The deposition of thin laminated (TL) and dark colored layers (D) in the Japan Sea during the late Quaternary was a nearly synchronous and basin-wide phenomenon (Tada et al., 1992, 1999; Nakajima et al., 1996). The base horizon of TL3/D3, top of TL2/D2, and base of TL1/D1 in KH-86-2-9 and KH-84-3-9 were chronologically designated as equivalent to those horizons in D-GC-6, respectively (Table 3).

In MD01-2409 four intervals are recognized based on visual lithologic description and soft X-ray radiography, which is an effective technique for analyzing sediment structures in detail and measuring relative density of sediment components (e.g., Hamblin, 1962): the core interval 4467–1820 cm consists of slump structures. Other notable features of this core are seen across the interval of 1820–1131 cm dated to 27.1–15.6 cal kyr BP, which is composed of olive gray colored homogeneous silty clay and includes many bivalve or single shells, shell fragments, sea urchins debris, and ice-rafted pebbles; the interval 1131–695 cm dated at 15.6–10.4 cal kyr BP, which includes three intervals of laminated clay at 1131–1030 cm corresponding to 15.6–13.7 cal kyr BP, 1019–968 cm to 13.5–13.0 cal kyr BP, and 861–695 cm to 11.3–10.4 cal kyr BP; the interval of 695–0 cm, which corresponds to 10.4–0 cal kyr BP, is composed of olive gray colored homogeneous silty clay and has burrows or bioturbation throughout the interval with intercalated thin layers of coarse-grained sand, volcanic ash and pumice fragments.

The age model (depths vs. calendar age) for core MD01-2409 was obtained from AMS ^{14}C dates for mixed planktonic foraminiferal tests at 15 levels, which were measured at the AMS facility of the Japan Atomic Energy Research Institute at Mutsu (Table 4). All the dates were corrected for a reservoir age ($\Delta R = 376 \pm 46$, + 400 years; $\Delta R = 0$) and converted to calendar years (cal kyr BP) using the Calib 4.3 software (Stuiver et al., 1998) for ^{14}C ages younger than 24 kyr BP and the second order polynomial equation of Bard (1998) for ^{14}C ages older than 24 kyr BP.

Multiple gravity core, 20 cm long, and the upper 74 cm in the piston core MR97-04-1, 683 cm long, were utilized for this study. MR97-04-1 is composed of olive gray colored homogeneous silty clay with intercalated thin layers of fine-grained and medium-grained sand or volcanic ash, and a thin laminated clay at 29.4 –28.7 m, corresponding to 17.9–17.6 cal kyr BP (Murayama et al., 1999).

Table 4
Chronostratigraphic framework (depth vs. calendar age) in MD01-2409

Reference no.	Depth (cm)	^{14}C age	Calendar age	Cal kyr BP
113	253.88	3978 ± 56	3401–3575	3.47
201	449.61	7944 ± 48	7947–8066	8.00
210–212	471.82	8463 ± 68	8416–8638	8.55
308	689.48	10020 ± 82	10197–10602	10.33
365–366	818.40	10689 ± 140	10850–10970	10.95
382–383	856.74	10639 ± 55	11096–11345	11.25
391–393	878.14	10895 ± 138	11308–11753	11.41
416	930.54	11293 ± 45	12269–12634	12.52
453–455	1015.57	12432 ± 78	13394–13702	13.50
487–488	1089.43	13355 ± 81	14032–14664	14.37
506	1128.28	13838 ± 130	15232–15989	15.58
621–622	1386.62	16688 ± 85	18564–19185	18.87
652	1452.11	17530 ± 143	19489–20198	19.84
707	1576.27	19325 ± 114	21541–22277	21.91
812	1810.66	23628 ± 63		26.89

The depth of 13.0 cm and 49.0–39.0 cm in the benthic $\delta^{18}O$ record of MR97-04-1 were correlated to the marine isotope stages (MIS) 2.0 and 3.0 of the standard $\delta^{18}O$ curve of Martinson et al. (1987) (Table 5). The difference between the values (about 0.5 ‰) of $\delta^{18}O$ for benthic foraminifera *Elphidium batilaris* recognized in the multiple gravity core and in the piston core suggests that some of the topmost sediment of the piston core, which corresponds to about 6 kyr duration, was lost in the coring process (Oba et al., 1999; Yamamoto, 1999). Marine isotope events (MIE) 2.0, 2.2, 3.0, and 3.3 at 222.5 cm in the piston core were used to construct the age model (depth vs. calendar age) in MR97-04-1 (Table 5).

Table 5
Chronostratigraphic framework (depth vs. calendar age) in MR97-4-1

Core	Depth (cm)	$\delta^{18}O$ (‰)		MI event	Cal kyr BP
		U. akitaensis	*E. batilaris*		
Gravity core	0.3	2.92	2.21		
	0.8	3.62	2.23		
	1.5	3.39	2.26		
	2.5	3.28	2.61		
	3.5	3.50	2.52		
	4.5	3.45	2.50		
	5.5	3.08	2.56		
	6.5	3.44			
	7.5	3.29	2.48		
	8.5	3.47	2.36		
	9.5	3.54	2.41		
	10.5	3.30	2.52		
	11.5	3.41			
	12.5	3.46	2.52		
	13.5	3.30	2.56		
	14.5	3.55			
	15.5	3.28	2.51		
	16.5	3.53			
	17.5	3.41	2.16		
	18.5	3.55	2.70		
	19.5	3.22	2.43		
Piston core	1.0	3.56	3.31		
	6.5		2.76		
	7.0	3.50	3.14		
	9.0	4.25	3.30		
	11.0	3.75	2.95		
	13.0	4.48	3.01	2.0	12.05
	18.5		2.70		
	19.0	4.59	3.84		
	22.0	4.86	3.91		
	25.0	4.81	3.66		
	28.0	5.03	4.26		
	29.3			2.2	17.85
	30.5	5.06	3.84		
	32.0	4.90			
	35.0	4.94	3.98		
	37.5	5.04	3.79		
	39.0	4.99	3.78		
	39.5			3.0	24.11
	49.0	4.55	3.54		
	59.0		3.66		
	69.0	4.56	3.57		
	222.5			3.3	50.21

3. Method of study

The average sampling intervals are; for D-GC-6 2.5 cm, which corresponds to 50–250 kyr throughout the core (Table A1); for KH-86-2-9 and KH-84-3-33 10 cm corresponds to 0.1 kyr (Tables A2 and A3); for KH-84-3-9 5 cm corresponds to 0.69 kyr (Table A4); for MD01-2409 16.5 cm corresponds to 0.25 kyr (Table A5); for gravity core 2.2 cm corresponds to 0.32 kyr and for piston core MR97-04-1 2.6 cm corresponds to 0.74 kyr (Table A6). (All data in Tables A1 –A6 is available online).

Diatom assemblages for each sample were examined by microscope. Paleoceanographic analyses were conducted through calculations of diatom abundance, relative abundance of extinct diatoms, ecological and biogeographical categories based on the habitats of diatom species, living warm-water and cold-water species, and diatom temperature estimates using the following relationship: $(Td' = [(Xw + \mathrm{XW})/(Xw + \mathrm{XW} + Xc + \mathrm{XC})] \times 100)$, where *Xw* is the frequency of warm-water species and *Xc* is that of cold-water species originally proposed by Kanaya and Koizumi (1966). We supplement *Xw* with several oceanic holoplanktonic and neritic–littoral holoplnktonic–meroplanktonic warm-water species, indicating as XW, and *Xc* with oceanic holoplanktonic cold-water species *Fragilariopsis oceanica*, indicating as XC. *Td′* values reflect more precisely oceanic holoplanktonic associations than originally proposed *Td* (Koizumi et al., 2004). Ecological and biogeographical subdivisions of diatom taxa are summarized in Table A7 (Koizumi et al., 2004). We also completed Q-mode factor analysis using all the diatom assemblage data except from core D-GC-6. The detailed procedures for slide-preparation, microscopic examination and Q-mode factor analysis are described in Koizumi et al. (2004).

4. Results

4.1. Chronostratigraphic analyses

4.1.1. Japan Sea side

The numbers of diatom valves in D-GC-6 increase from 8.0 cal kyr BP to the top of the core with the highest abundances of 11.7×10^7 at 2.03 cal kyr BP (Fig. 2). They largely fluctuate at intervals of ~4-kyr in the glacial

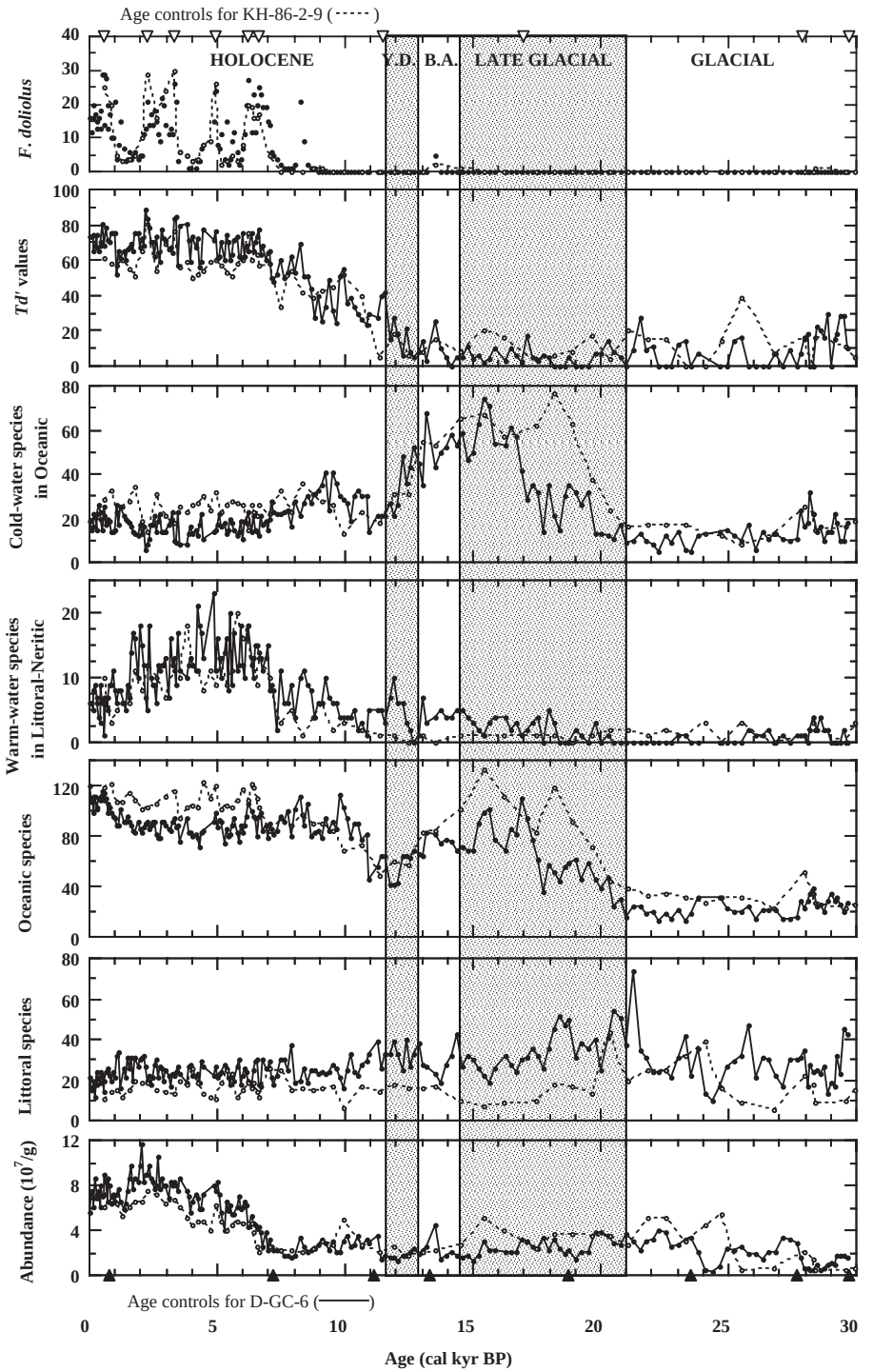

Fig. 2. Chronostratigraphic variations of *Fragilariopsis doliolus*, Td′ values, ecological and biogeographical diatom categories, and paleoceanographic categories (valves/200 valves), and diatom abundance ($\times 10^7$ valves/dry g of sediment) in D-GC-6 (solid) and KH-86-2-9 (dotted). Black triangles are age controls for D-GC-6 and white triangles for KH-86-2-9. Chronostratigraphic subdivision is shown in figure. Y.D.=Younger Dryas cooling, B.A.=Bolling/Allerod interstadial.

and late glacial interval, ~2-kyr in the Bolling/Allerod to the early Holocene and ~1-kyr in the Holocene. Extinct and freshwater diatoms are not common throughout the core (Table A1). The relative abundance of littoral species decreases gradually from 22.0 cal kyr BP. The relative abundance of oceanic species increases from the bottom to the top of the core, but decreases during the period of the last glacial maximum and Younger Dryas cooling. The relative abundance of littoral–neritic, warm-water species increases after 10.5 cal kyr BP and reaches 11.5% at 4.9 cal kyr BP and then decreases to 3.0% at the top. Oceanic cold-water species rapidly increase in relative abundance during the period from 19.5 to 15.4 cal kyr BP and then decrease until 11.0 cal kyr BP. The diatom temperature (*Td′*) values increase during the period of 14.0–7.0 cal kyr BP. The relative abundance of the TWC indicator species *Fragilariopsis doliolus* largely fluctuates at ~1.5-kyr intervals after an abrupt appearance at 8.3 cal kyr BP.

The diatom abundance in KH-86-2-9 increases from the bottom to the top of the core (Fig. 2). There is a peak in the littoral species from between 25.0–20.5 cal kyr BP, but it decreases suddenly at 20.5 cal kyr BP and maintains an average of ~15% thereafter. The oceanic species have a low abundance up to 20.5 cal kyr BP, then increases to 15 cal kyr BP, declines to ~10.0 cal kyr BP, and remains constant thereafter. The relative abundance curve of oceanic species is almost a mirror image of the curve of littoral species, showing an increase at 20.5–15.5 cal kyr BP in KH-86-2-9. The relative abundance of littoral–neritic, warm-water species increases from 8.0 to 6.0 cal kyr BP and then decreases. The oceanic cold-water species dominate in terms of relative abundance from between 18.0–13.0 cal kyr BP, but after 7.5 cal kyr BP, the warm-water species dominate. Since 10.0 cal kyr BP, the *Td′* values fluctuate on a periodicity of ~1.5-kyr, and this reflects the relative abundance of major oceanic warm-water species (see Table A7).

The average number of diatom valves in KH-84-3-33 is larger than that in KH-84-3-9 which is located further off shore (Figs. 1 and 3). Large fluctuations at ~1.5-kyr intervals occur in KH-84-3-33 with secondary and smaller fluctuations between them. High values appear at 9.3, 6.5, and 3.5 cal kyr BP in KH-84-3-9.

In core KH-84-3-33, fluctuations in the range of 15–48 (valves/200 valves) in the relative abundance of littoral species occur at ~1.0-kyr intervals with secondary and smaller fluctuations (Fig. 3). The relative abundance of extinct diatoms, which are composed of *Neodenticula kamtschatica* and *Thalassiosira antiqua,* increases gradually up to 12.0 cal kyr BP during the late glacial phase of KH-84-3-9 (Table A3). However, littoral diatoms are uncommon throughout the core, especially in KH-84-3-9. The relative abundance of littoral–neritic diatoms decreases from ~7.0 cal kyr BP in KH-84-3-33 and 13.0 cal kyr BP in KH-84-3-9 to the top, and fluctuate at ~1.5-kyr intervals with secondary and smaller fluctuations. The relative abundance curve of oceanic species is almost a mirror image of that of littoral–neritic species.

The littoral–neritic cold-water species are very rare and warm-water species are not common throughout both cores (Tables A2 and A3). The relative abundance of oceanic warm-water species is dominant over the cold-water ones and fluctuates at ~1.5-kyr intervals. The *Td′* values and relative abundances of *F. doliolus* in KH-84-3-33 vary in dominance and fluctuate after ~7.0 cal kyr BP (Fig. 3). On the other hand, in KH-84-3-9 the relative abundance of oceanic cold-water species dominates until 6.5 cal kyr BP, after which the dominance alternates between cold-water species and warm-water species at ~1.5-kyr intervals.

4.1.2. Northwest Pacific side

Since 27.0 cal kyr BP the average number of diatom valves in MD01-2409 is slightly greater than that in MR97-04-1 (Fig. 4). High values in MD01-2409 are recognized at 14.8–12.6 and 10.8–10.6 cal kyr BP. These abundance peaks correspond to peaks of biogenic opal content, which occur in the laminated intervals (Fig. 7). Large fluctuations occur with secondary and smaller fluctuations at ~1.0-kyr intervals (Fig. 4).

The relative abundance of extinct diatoms in both MD01-2409 and MR97-04-1 decreases from the bottom of these cores to 15.0–13.0 cal kyr BP. Extinct diatoms are very low in abundance in the upper part of MD01-2409, but in MR97-04-1 they increase slightly, peaking at 9.7, 6.6, and 6.3 kyr BP. Extinct diatoms *Melosira albicans* and *Pseudopodosira elegans* are dominant throughout the lower part in two cores, corresponding to the glacial phase.

Freshwater and littoral diatoms are not common throughout both cores (Tables A5 and A6). The relative abundance of littoral diatoms gradually increases in the cores. *Stephanopyxis turris* and *Thalassionema nitzschioides* are dominant throughout the cores. Oceanic diatoms increase in the relative abundance at 15.0–12.0 cal kyr BP. The relative abundance curve of oceanic species is almost a mirror image of the curve of littoral–neritic species.

In littoral–neritic and oceanic associations, the cold-water species dominate in relative abundances over warm-water ones throughout both cores. The relative

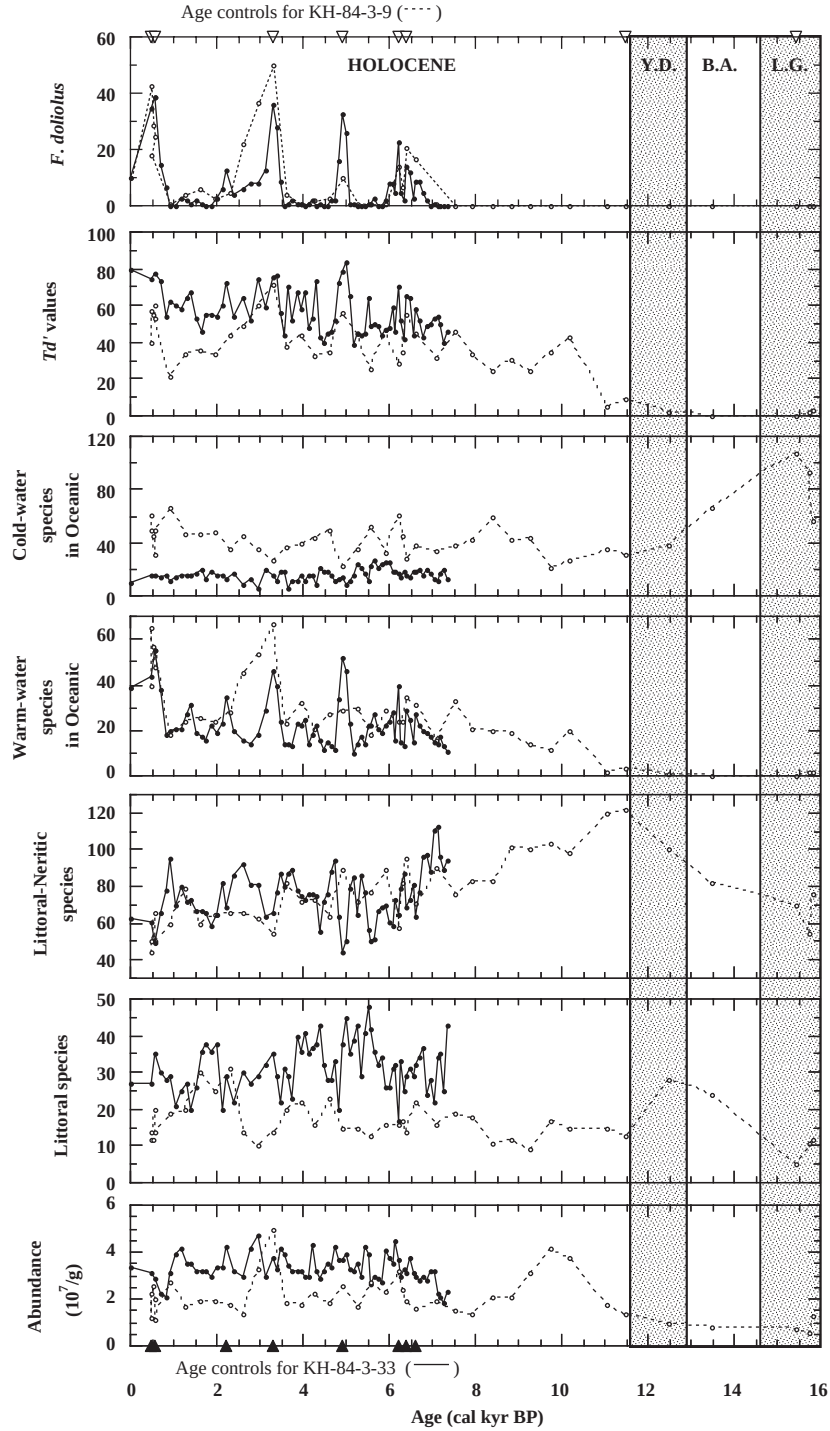

Fig. 3. Chronostratigraphic variations of *Fragilariopsis doliolus*, Td′ values, ecological and biogeographical diatom categories, and paleoceanographic categories (valves/200 valves), and diatom abundance in KH-84-3-33 (solid) and KH-84-3-9 (dotted). Black triangles are age controls for KH-84-3-33 and white triangles for KH-84-3-9. Chronostratigraphic subdivision is shown in figure. Y.D=Younger Dryas cooling, B.A.=Bolling/Allerod interstadial, L.G.=Late Glacial.

abundance of littoral–neritic cold-water species rapidly increases at ~10.0 cal kyr BP in MD01-2409 and at 6.5 cal kyr BP in MR97-4-1 (Fig. 4). The relative abundance of a littoral–neritic cold-water *Odontella aurita*, which was originally defined as an oceanic cold-water (*Xc*) species (Kanaya and Koizumi, 1966), fluctuates

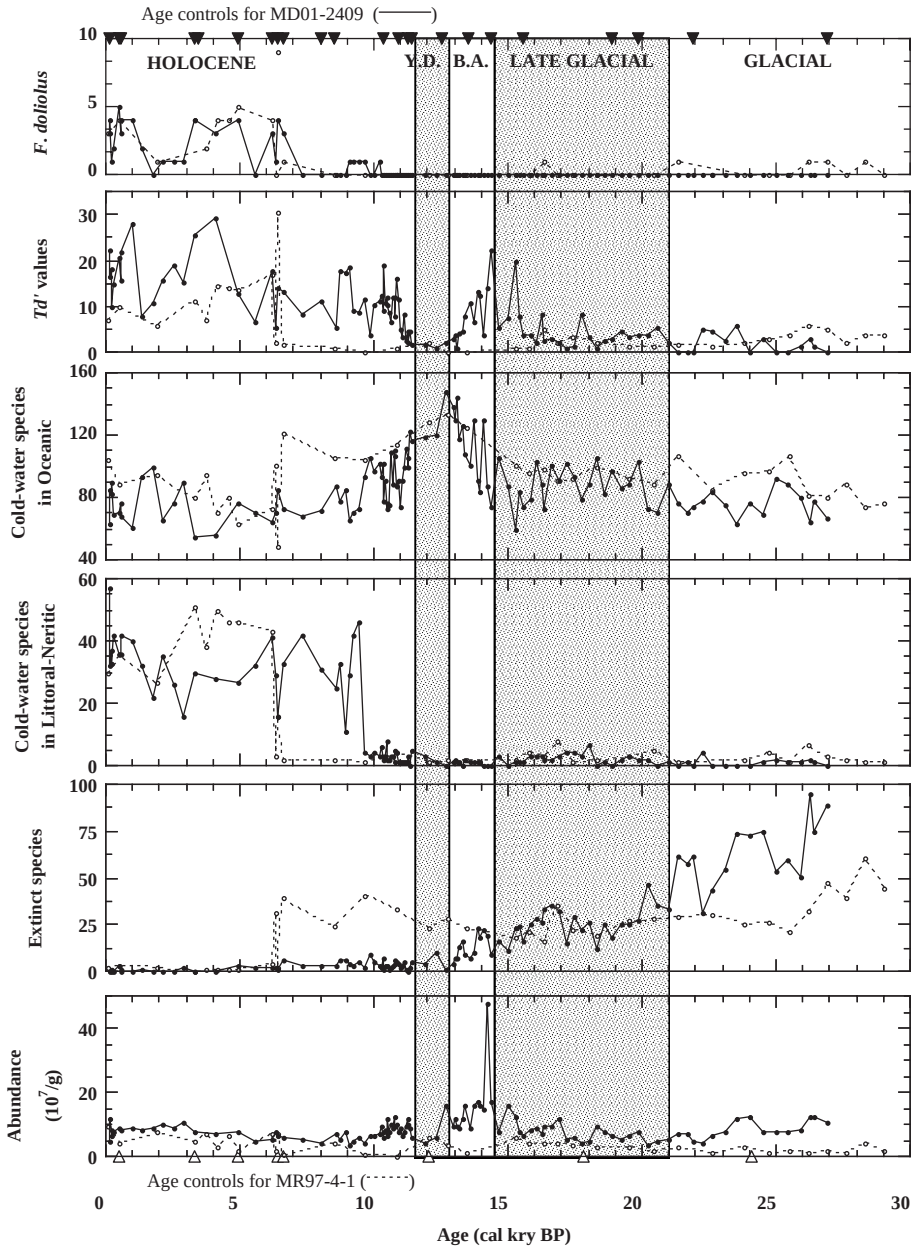

Fig. 4. Chronostraigraphic variations of *Fragilariopsis doliolus*, Td′ values, ecological and biogeographical diatom categories, and paleoceanographic categories (valves/200 valves), and diatom abundance in MD01-2409 (solid) and MR97-04-1 (dotted). Black triangles are age controls for MD01-2409 and white triangles for MR97-04-1. Chronostratigraphic subdivision is shown in figure. Y.D.=Younger Dryas cooling, B.A.=Bolling/Allerod interstadial.

considerably in the upper part of both cores. The oceanic cold-water species gradually increase from the bottom of the cores until 12.5 cal kyr BP and then decrease to 6.0 cal kyr BP in both cores. The increases in *Td′* values occur at 15.6–13.7 and 11.3–10.3 cal kyr BP, and correspond to the laminated intervals, which are due to the increase of the warm-water species *Thalassiosira leptopus* and the decrease of the cold-water species. Since 12.0 cal kyr BP, the *Td′* values increase cyclically. The relative abundance of *F. doliolus* increases cyclically since 7.5 cal kyr BP.

4.2. Q-mode factor analysis

The highest six factors in five cores explain ~90.3% of the total variance (Table 6). Taxa with the top 20

Table 6
Variance explained by six significant factors

Factor	1	2	3	4	5	6
% of variance explained	47.93	14.40	9.33	9.14	7.19	2.32
Cumulative % of variance explained	47.93	62.33	71.65	80.79	87.99	90.31

high scores for each factor are shown in Table 7 and chronostratigraphic variation of each factor loading in each core is shown in Figs. 5, 6.

Factor 1 is composed exclusively of a cosmopolitan, predominantly neritic holoplanktonic species *Thalassionema nitzschioides*, which shows a very high positive score. This species is a common, widely spread, and neritic northern temperate species, often found in great numbers in coastal locations around the Japanese Islands, especially in winter and spring (Takano, 1990). On the other hand, Sancetta et al. (1992) observed the abundance of *Tn. nitzschioides* during the spring bloom off Oregon, northeast Pacific Ocean. The species also increased offshore and coincided with the occurrence of displaced benthic diatoms during 30–11 kyr BP.

Factor 2 is dominated by *Thalassiosira nordenskioldii*, which is one of the most abundant arctic species, often occurring in enormous numbers.

Factor 3 is predominated by the littoral–neritic, tychopelagic, cold-water species *Odontella aurita*. This species has wide distribution, but flourishes most in arctic and boreal seas, especially during April and May. The increased abundances of *O. aurita* in the sediments may represent a local increase in productivity occurring in the areas along the frontal zone between coastal and offshore water (Sancetta, 1982), as supported by the fact that it is abundant in Holocene sediments of the Northwest Pacific Ocean but very rare in the Japan Sea and Okhotsk Sea Holocene sediments.

Factor 4 is dominated by subarctic species such as *Fragilariopsis oceanica*, *Thalassiosira gravida* and *Thalassiosira trifulta*. *Fragilariopsis oceanica* is recognized in sea-ice, which reached the coast of Abashiri on the Okhotsk Sea (Shiga and Koizumi, 2000). *Thalassiosira gravida* and *T. trifulta* do not extend as far north as *T. nordenskioldii*, and thrive in cold, productive waters (Sancetta, 1982).

Factor 5 is predominated by extinct species *Melosira albicans*, which was originally described at the Pliocene Ust-Kamtschatica, on the east side of Kamchatka Peninsula (Sheshukova-Poretskaya, 1964).

Factor 6 is dominated by the TWC indicator species *F. doliolus*. The second component is *Coscinodiscus marginatus,* which was originally defined as an oceanic cold-water species (*Xc*) by Kanaya and Koizumi (1966), but is abundant in association with *F. doliolus* in the surface sediments from the southeastern part of the Japan Sea.

4.2.1. Japan Sea side

The fluctuations of Factor 4 (Fig. 5) bear a very close resemblance to the relative abundance curve of the oceanic cold-water species (Fig. 2). Factor 6 consists of two intervals, in which *C. marginatus* dominates in pre-Holocene and *F. doliolus* dominates in Holocene (Tables A2 and A4). The fluctuation patterns recognized in Factor 1, Factor 3 and Factor 4 are almost mirror images of the patterns in Factor 2, Factor 6 and Factor 5, respectively.

Each factor shows sharp fluctuations during the interval at 16.0–13.0 cal kyr BP. After 7.0 cal kyr BP, the fluctuation pattern of Factor 6 resembles the relative abundance curve of *F. doliolus* (Figs. 2 and 3). Each factor, especially Factors 1 and 2, fluctuates at ~1.3-kyr intervals (Fig. 5).

4.2.2. Northwest Pacific side

The fluctuations of Factors 3 and 5 very closely resemble the temporal abundance variations of the littoral–neritic, cold-water species and extinct diatoms (Figs. 4 and 6). The fluctuation pattern of Factor 1 and Factor 4 are almost mirror images of the patterns of Factor 2 and Factor 6, respectively.

Factor 4 and Factor 5 increase but Factor 2 decreases during the interval from 19.0 to 15.5 cal kyr BP. Factor 1 and Factor 4 increase but Factor 2 and Factor 6 decrease at 13.0–11.5 cal kyr BP, and after 9.5 cal kyr BP Factor 3 increases but Factor 2 decreases.

5. Discussion

5.1. Paleoceanography around the Tsugaru Strait

5.1.1. Japan Sea side

The dominance of littoral and extinct diatoms during the interval of 25.0–20.0 cal kyr BP (Fig. 2, and Tables A1 and A2) reflect a fall in sea level, increased freshwater input into the Japan Sea and the development of stratification in the water column (Oba et al., 1991; Ishiwatari et al., 1999). Increases in the oceanic cold-water species (Factors 2 and 4) at 20.0–11.5 cal kyr BP indicates a flow of the Oyashio water into the Japan Sea

Table 7
Scores of 20 diatom species in each factor

Factor 1		Factor 2		Factor 3		Factor 4		Factor 5		Factor 6	
Score	Taxa	Score	Taxa	Score	Taxa	Score	Taxa	Score	Taxa	Score	Taxa
0.89	*Thalassionema nitzschioides*	0.90	*Thalassiosira nordenskioldii*	0.88	*Odontella aurita*	0.53	*Fragilariopsis oceanica*	0.89	*Melosira albicans*	0.63	*Fragilariopsis doliolus*
0.15	*Coscinodiscus marginatus*	0.23	*Thalassionema nitzschioides*	0.34	*Neodenticula seminae*	0.44	*Thalassiosira gravida*	0.21	*Thalassiosira gravida* v.	0.39	*Coscinodiscus marginatus*
0.12	*Fragilariopsis doliolus*	0.16	*Thalassiosira hyalina*	0.21	*Thalassiosira gravida*	0.43	*Thalassiosira trifulta*	0.15	*Thalassiosira nordenskioldii*	0.24	*Thalassiosira trifulta*
0.11	*Thalassiosira oestrupii*	0.10	*Thalassiosira leptopus*	0.17	*Thalassionema nitzschioides*	0.23	*Bacteriosira fragilis*	0.13	*Fragilariopsis cylindrus*	0.21	*Thalassiosira nordenskioldii*
0.11	*Thalassiosira linetus*	0.09	*Thalassiosira pacifica*	0.09	*Thalassiosira leptopus*	0.21	*Stephanophyxis turris*	0.12	*Bacteriosira fragilis*	0.21	*Neodenticula seminae*
0.10	*Delphineis surirella*	0.09	*Thalassiosira* spp.	0.07	*Porosira gracilis*	0.18	*Thalassiosira gravida* v.	0.10	*Fragilariopsis doliolus*	0.17	*Thalassiosira oestrupii*
0.08	*Odontella sinensis*	0.08	*Fragilariopsis cylindrus*	0.05	*Paralia sulcata*	0.18	*Pseudopodosira elegans*	0.08	*Thalassionema nitzschioides*	0.17	*Odontella sinensis*
0.08	*Thalassiothrix longissima*	0.06	*Thalassiosira antiqua*	0.04	*Thalassiosira nordenskioldii*	0.15	*Stephanopyxis* spp	0.08	*Fragilariopsis oceanica*	0.13	*Thalassiothrix frauenfeldii*
0.08	*Thalassiothrix frauenfeldii*	0.05	*Thalassiosira decipiens*	0.03	*Fragilariopsis cylindrus*	0.14	*Coscinodiscus marginatus*	0.08	*Thalassiosira linetus*	0.12	*Thalassiothrix longissima*
0.07	*Ditylum brightwellii*	0.03	*Thalassiosira lacustris*	0.03	*Actinocyclus curvatulus*	0.13	*Neodenticula seminae*	0.07	*Thalassiosira hyalina*	0.12	*Rhizosolenia styliformis*
0.06	*Rhizosolenia styliformis*	0.03	*Neodenticula seminae*	0.03	*Rhizosolenia styliformis*	0.11	*Thalassiosira* cf. *Allenii*	0.06	*Delphineis surirella*	0.11	*Ditylum brightwellii*
0.06	*Azpeitia tabularia*	0.02	*Porosira gracilis*	0.02	*Fragilariopsis doliolus*	0.09	*Fragilariopsis cylindrus*	0.05	*Pseudopodosira elegans*	0.11	*Thalassiosira linetus*
0.06	*Thalassiosira pacifica*	0.02	*Thalassiosira ferelineata*	0.02	*Thalassiosira linetus*	0.09	*Thalassionema nitzschioides*	0.04	*Odontella aurita*	0.08	*Actinoptychus senarius*
0.06	*Actinoptychus senarius*	0.02	*Thalassiosira* cf. *Allenii*	0.02	*Thalassiosira* spp.	0.08	*Actinocyclus curvatulus*	0.04	*Thalassiothrix frauenfeldii*	0.07	*Delphineis surirella*
0.05	*Nitzschia bicapitata*	0.01	*Cocconeis scutellum*	0.02	*Rhizosolenia setigera*	0.08	*Thalassiosira hyalina*	0.03	*Thalassiosira pacifica*	0.06	*Nitzschia interruptastriata*
0.04	*Pseudosolenia calcar-avis*	0.00	*Actinocyclus curvatulus*	0.02	*Bacteriosira fragilis*	0.07	*Thalassiosira antiqua*	0.03	*Nitzschia bicapitata*	0.06	*Pseudosolenia calcar-avis*
0.04	*Thalassiosira eccentirca*	0.00	*Actinocyclus ochotensis*	0.01	*Thalassiosira eccentirca*	0.07	*Neodenticula kamtschatica*	0.03	*Cocconeis costata*	0.06	*Stellarima stellaria*
0.04	*Stellarima stellaria*	0.00	*Cyclotella striata*	0.01	*Cyclotella striata*	0.07	*Thalassiosira decipiens*	0.03	*Cocconeis scutellum*	0.05	*Actinocyclus curvatulus*
0.03	*Thalassiosira trifulta*	0.00	*Amphora* spp.	0.01	*Nitzschia interruptastriata*	0.06	*Thalassiosira ferelineata*	0.02	*Thalassiosira* cf. *Allenii*	0.05	*Azpeitia tabularia*
0.03	*Thalassiosira ferelineata*	0.00	*Cocconeis costata*	0.01	*Actinoptychus senarius*	0.06	*Melosira albicans*	0.02	*Thalassiosira decipiens*	0.05	*Rhizosolenia setigera*

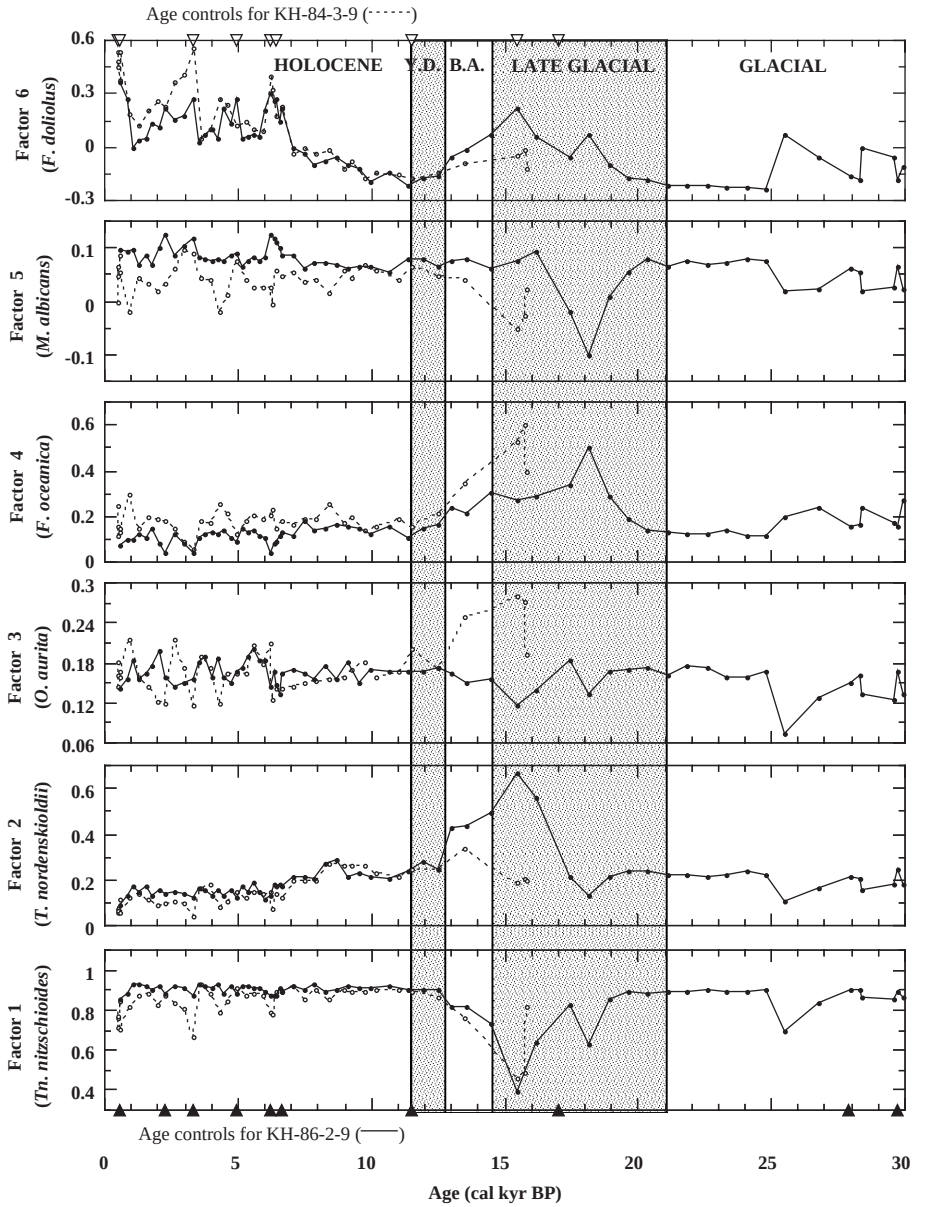

Fig. 5. Chronostratigraphic variations of the loadings for each factor in Q-mode factor analysis of the diatom flora in KH-86-2-9 (solid) and KH-84-3-9 (dotted). Black triangles are age controls for KH-86-2-9 and white triangles for KH-84-3-9. Chronostratigraphic subdivision is shown in figure. Y.D.=Younger Dryas cooling, B.A.=Bolling/Allerod interstadial.

through the Tsugaru Strait caused by the baroclinic component, which is supported by the horizontal density gradient, at the Strait (Ikeda et al., 1999). The intrusion of Oyashio water which propagated south from the Strait at 20 cal kyr BP (KH-86-2-9) is even evidenced at core site D-GC-6 at 17.5 cal kyr BP (Fig. 2). The peak in loading of Factor 4, which is mainly composed of the subarctic sea-ice species, at ~18.0 cal kyr BP shifts to a peak of Factor 2, a more northern arctic species, at ~15.0 cal kyr BP (Fig. 5). The same event occurred also from 18.0–17.0 cal kyr BP to 14.0–13.0 cal kyr BP in the Northwest Pacific side of the Tsugaru Strait (Fig. 6). After 11.5–9.0 cal kyr BP in early Holocene, the littoral–neritic, warm-water species, including mainly *Azpeitia tabularia* and *Nitzschia interruptastriata*, and *F. doliolus* are dominant.

The TWC in the Japan Sea is evidenced by the increase of *Td′* values after ~11.0 cal kyr BP and by that the fluctuations of *F. doliolus* occur after 8.8 cal kyr BP (Figs. 2 and 3). The fluctuations at the ~1.5-kyr

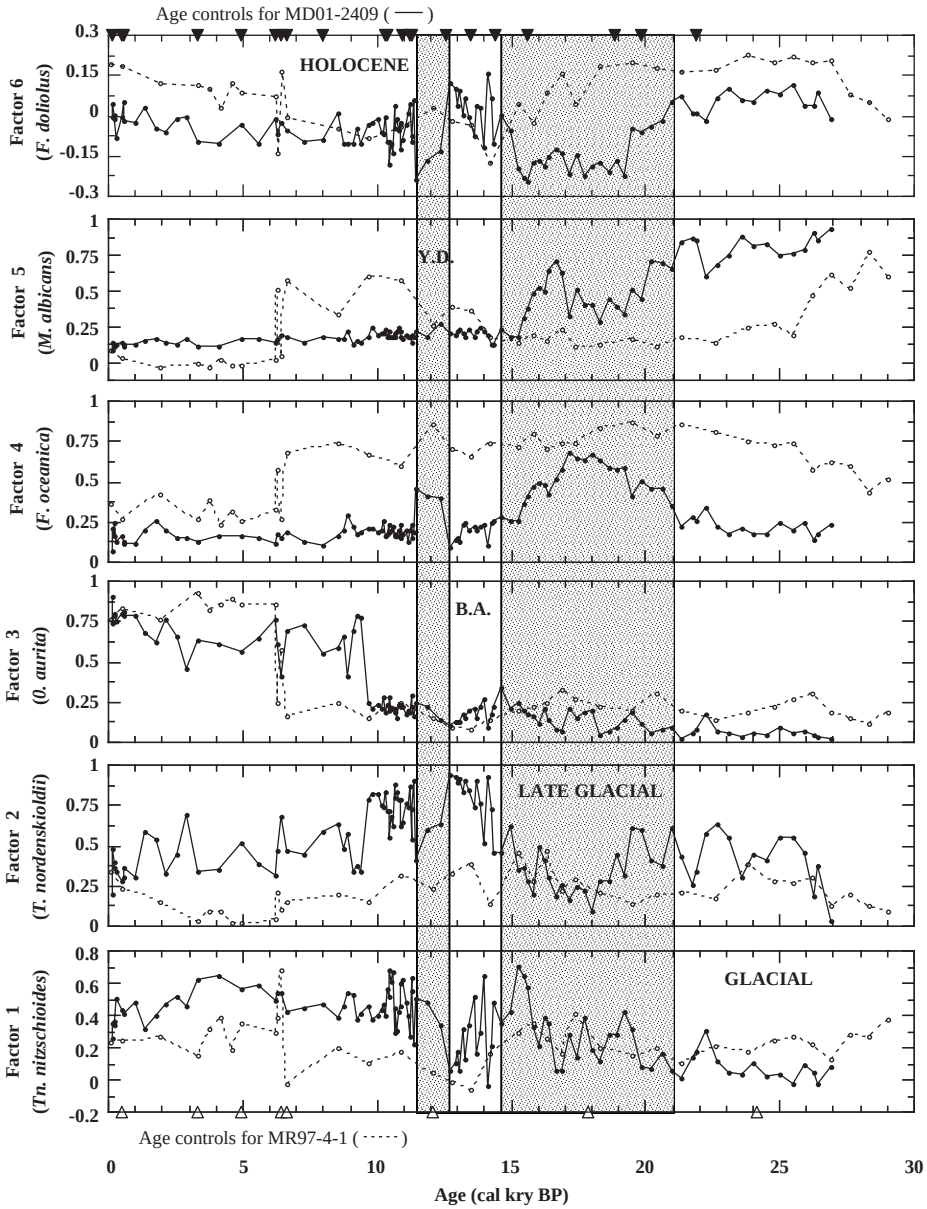

Fig. 6. Chronostratigraphic variations of the loadings for each factor in Q-mode factor analysis of the diatom flora in MD01-2409 (solid) and MR97-04-1 (dotted). Black triangles are age controls for MD01-2409 and white triangles for MR97-04-1. Chronostratigraphic subdivision is shown in figure. Y.D.=Younger Dryas cooling, B.A.=Bolling/Allerod interstadial.

intervals in the relative abundance of *F. doliolus* can be correlated with those recognized in the Soya Warm Current, which starts in the Japan Sea and flows north as the Northward Current and reaches the Soya Strait (Shimada et al., 2000, 2004).

There is a shift in the dominance of cold-water diatom species in the last glacial period to warm-water ones in the present interglacial during the period from 10.0 cal kyr BP to 7.0 cal kyr BP. The relative abundance of littoral–neritic, warm-water species increases from 10.5 to 4.9 cal kyr BP. Takei et al. (2002) documented that a branch of the Oyashio Current continued to flow into the Japan Sea through the Tsugaru Strait until 4.8 cal kyr BP and coexisted with the TWC in the Japan Sea between 8.3 and 4.8 cal kyr BP. They argue that a modern oceanographic regime has prevailed since 4.8 cal kyr BP.

The cooling event from 4.8 to 3.5 cal kyr BP, which is indicated by the remarkable decreases of *F. doliolus* and the *Td′* value (Figs. 2, 3), might be related to the

Pulleniatina minimum event in the East China Sea from 4.5 to 3.0 cal kyr BP, which is proposed to be due to a cooling event or a suppression of the Kuroshio (Warm) Current (Jian et al., 1996; Li et al., 1997).

The cooling event at 2.8–1.3 cal kyr BP (Figs. 2, 3) is more remarkable in the northern site than in the southern site. A cooling event at ~2.0 cal kyr BP is also recognized in the Okhotsk Sea, with associated fluctuations in the extent of sea-ice during the interval from 1.8 to 1.3 cal kyr BP (Gorbarenko et al., 2002; Koizumi et al., 2003). However, the Jomon–Yayoi warm stage and Yayoi transitional stage are recognized at ~2.0 cal kyr BP in Honshu Island (Sakaguchi, 1982, 1983), which leads to the climatic differentiation that had been developing in the northern Japan Sea area.

5.1.2. Northwest Pacific side

Reworked and displaced extinct diatoms are common during the last glacial time when sea level was lower. The high *Td′* values at 15.6–13.0 cal kyr BP in MD01-2409 correspond to the Bolling/Allerod interstadial. This is similar to the time interval ~14.6–12.9 cal kyr BP, assigned to the low-oxygen conditions and laminated sediment deposition during periods of warm climate at ODP Hole 893A in the Santa Barbara basin off southern California (Kennett and Ingram, 1995) and to the warm climate at ODP Site 1019 off northern California (Barron et al., 2003) (Fig. 4). Subarctic sea-ice species (Factor 4), which dominated at 21.0–15.0 cal kyr BP, shifted to the arctic species (Factor 2) at 14.2–12.6 cal kyr BP (Fig. 6). The remarkable decreases of Factors 2 and 6, but increase of Factor 4 at 12.5–11.2 cal kyr BP correspond to the Younger Dryas cooling event.

The decrease of oceanic cold-water species after the Younger Dryas cooling is symptomatic of more general global warming. The abrupt and remarkable increase of littoral–neritic cold-water species *Odontella aurita*, which occurs for the first time at 9.5–9.0 cal kyr BP, suggests the southward intrusion of the Oyashio Current along the eastern margin of Hokkaido and Honshu Island. Since then, the modern hydrographic mode has prevailed in the Northwest Pacific Ocean.

The relative abundances of the TWC indicator species *F. doliolus* are almost equivalent in D-GC-6, KH-86-2-9, and KH-84-3-33 (under the TWC), and KH-84-9 (under the Northward Current), but it is very much smaller in MD01-2409 (under the Tsugaru Warm Current).

Fragilariopsis doliolus first occurs at ~10.0 cal kyr BP in the Northwest Pacific side of the Tsugaru Strait (Fig. 4). In the Japan Sea, *F. doliolus* first occurs at 13.6 cal kyr BP and fluctuates after 8.8 cal kyr BP at D-GC-6 (Fig. 2). During the early Holocene from 11.2 to 8.8 cal kyr BP, the TWC flowed intermittently into the Japan Sea through the Tsushima Strait, but after 8.8 cal kyr BP the TWC continuously entered the Japan Sea (Oba et al., 1991). According to Koizumi et al. (2004) *F. doliolus* is recognized to occur continuously off Kashima (36.0°N, 141.5°E) since 10.0 cal kyr BP. *F. doliolus* is also recognized to occur sporadically after 144.0 and after 90.0 cal kyr BP off Sanriku (38.9°N, 143.4°E) (Shimada and Hasegawa, 1999). Both results suggest that occurrences of *F. doliolus* earlier than ~8.8 cal kyr BP were due to northward expansion of the Kuroshio Current. Formation of the Tsugaru Warm Current through the Tsugaru Strait as permanent feature is assumed to have occurred later than ~8.8 kyr BP, as the cyclic occurrences of *F. doliolus* indicate (Table 3, Figs. 2–4).

5.2. Thinly laminated layers

5.2.1. Japan Sea side

The thinly laminated layers in the Japan Sea, including TL3 (27.9 to 25.4 cal kyr BP) and TL2 (23.8–17.0 cal kyr BP) are characteristic sediments of the Japan Sea, where they are considered to have formed under paleoenvironmental conditions typified by a lower sea-level and lower salinity, enhanced stratification of the water column, and severe euxinic bottom water conditions (Nakajima et al., 1996; Tada et al., 1999; Ishiwatari et al., 1999).

The first thinly laminated layer (TL1) at 11.5–11.0 cal kyr BP contains a lot of foraminiferal tests and consists of fine parallel laminae (Ikehara, 2003). These three laminated layers are considered synchronous in the Japan Sea (Tada et al., 1992).

5.2.2. North Pacific side

Thinly laminated layers, especially those in the Bolling/Allerod phase of the cores, include abundant diatom valves and a high biogenic opal content (Fig. 7). The layers coincide with high *Td′* values due to the combination of an increase in the relative abundance of the warm-water species *Thalassiosira leptopus* and the lower occurrence of cold-water species, leading to the conclusion that they formed during a warm phase in the last global deglaciation (Figs. 4 and 7). According to Narita et al. (2002), the productivity of biogenic opal during the warmer periods was higher than during colder periods in the northwestern Pacific Ocean.

The chronologic subdivisions of MD01-2409 can be correlated with the climatic succession from the late

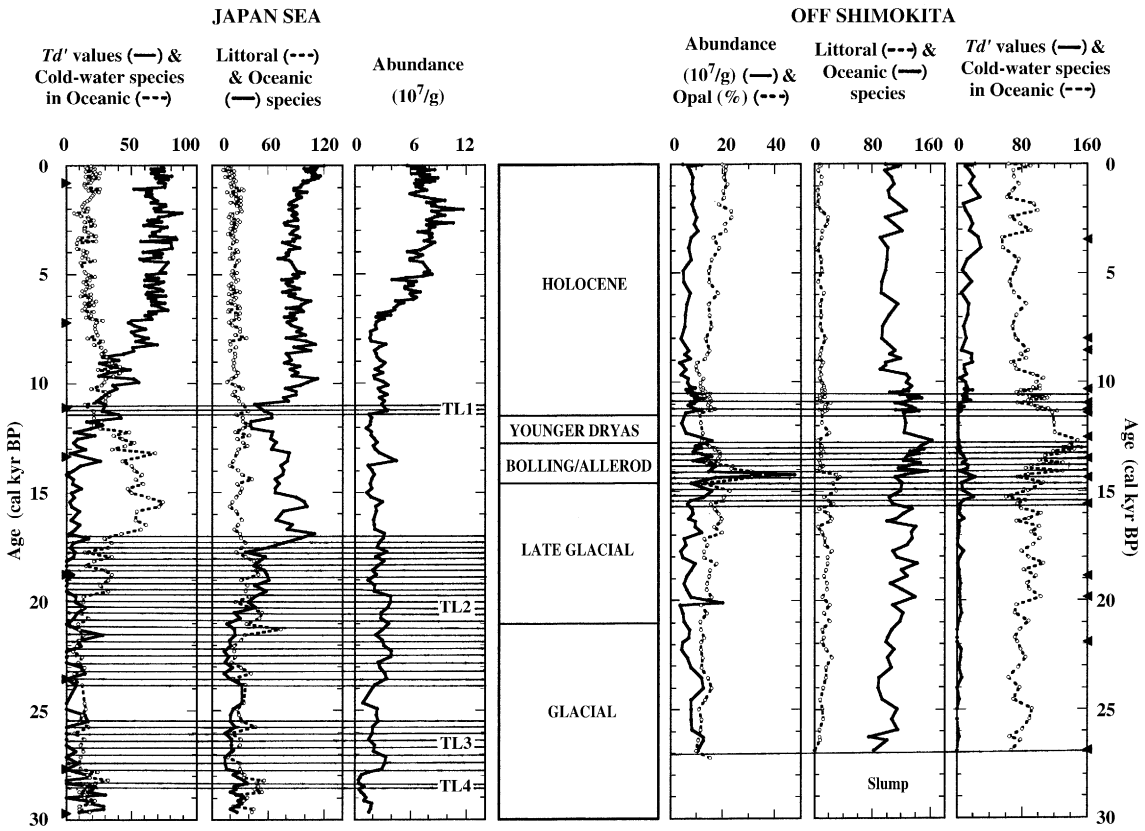

Fig. 7. Comparision of thinly laminated layers (stripe) between the Japan Sea (D-GC-6) and off Shimokita in the Northwest Pacific Ocean (MD01-2409) based on sedimentary environment and paleoclimatic subdivision (Kennett and Ingram, 1995; Barron et al., 2003). Black triangles are age controls for each core, respectively (Tables 2 and 4).

glacial interval (21.0–14.6 cal kyr BP) to the Bolling/Allerod interstadial (14.6–12.9 cal kyr BP), to the Younger Dryas cooling (12.9–11.6 cal kyr BP), and to the Holocene (11.6–0 cal kyr BP) (Kennett and Ingram, 1995; Barron et al., 2003). Global meltwater pulses 1A (~14.2 cal kyr BP) and 1B (~11.3 cal kyr BP) caused a decrease in oceanic cold-water species (Fairbanks, 1990). The deglacial rise in sea level and influx of underlying Oyashio water after 10.4 cal kyr BP did not allow the formation of laminated layers.

5.3. Paleoenvironmental changes around the Tsugaru Strait

The hydrographic environmental changes around the Tsugaru Strait based on the diatom analysis are summarized as follows:

5.3.1. 30.0–20.0 cal kyr BP

A fall in sea level associated with eustatic sea level changes and the intensification of the Oyashio Current caused erosion of submarine sediments in the near shore region of eastern area of the Tsugaru Strait. At the same time, the fall in sea level and the inflow of a colder less-saline oceanic water mass into the Japan Sea led to stratification of the water column producing thinly laminated layers in the Japan Sea (Nakajima et al., 1996; Tada et al., 1999; Ishiwatari et al., 1999).

5.3.2. 20.0–9.5 cal kyr BP

Oyashio water flowed into the Japan Sea through the Tsugaru Strait at 20.0 cal kyr BP and propagated from around the strait to the area around the Oki Ridge at 17.5 cal kyr BP. A cooling was increasingly intensified around the Tsugaru Strait after ~15.0 cal kyr BP when a cold subarctic water mass with sea-ice was replaced by an arctic water mass. The Younger Dryas cooling event is recorded in MD01-2409 on the Pacific side of the Tsugaru Strait by an abrupt increase in Factor 6 (*F. doliolus*) and Factor 2 (*T. nordenskioldii*) and abrupt increase in Factor 4 (*F. oceanica*) (Fig. 6). Presumably, this indicates an increase in sea-ice at this time off northwest Japan. In the Japan Sea, however, no clear changes in these factors are apparent during the Youn-

ger Dryas (Fig. 5). Also, oceanic cold-water species decline abruptly in abundance during the Younger Dryas in cores KH-86-2-9 and D-GC-6, while *Td′* values are rising (Fig. 2), suggesting decreasing incursion of cold Oyashio waters through the Tsugaru Strait. The primary expression of the Younger Dryas in the Japan Sea appears to have been the cessation of deposition of laminated sediments apparently caused by increased oxygen levels in bottom waters.

5.3.3. 9.5–0 cal kyr BP

Oyashio water subsided in the mixed water region of the Oyashio and Kuroshio off northeast Japan after 9.5 cal kyr BP. The modern mode, represented by 1.5-kyr fluctuations in the TWC, was established after a transitional phase from 9.5 to 7.0 cal kyr BP in the Japan Sea.

6. Conclusion

1. Increasing of oceanic cold-water diatom species around the Tsugaru Strait at 20.0–11.5 cal kyr BP indicates a flow of the Oyashio water into the Japan Sea through the Tsugaru Strait.
2. Oceanic cold-water species, including subarctic sea-ice species (Factor 4) and arctic species (Factor 2), have peaks in their relative abundances at 18.0–17.0 cal kyr BP and 15.5–12.5 cal kyr BP, respectively.
3. The Younger Dryas cooling event at 12.9–11.6 cal kyr BP was clearly recorded by the mass occurrence of oceanic cold-water species in the eastern area of the Tsugaru Strait, but not in the Japan Sea.
4. Warming surrounding the Younger Dryas cooling event at 15.6–13.0 cal kyr BP and 11.6–10.3 cal kyr BP led to the development of thinly laminated layers off Shimokita in the eastern area of the Tsugaru Strait.
5. Oyashio water intruded into deeper depths in the mixed water region off Sanriku since 9.5 cal kyr BP. The fluctuation of the TWC system at 1.5-kyr intervals developed after 9.5–7.0 cal kyr BP around the Tsugaru Strait.
6. The relative abundance of *Fragilariopsis doliolus* is almost equivalent in the cores from the TWC and the Northward Current, but it is much smaller in the Tsugaru Warm Current.

Acknowledgements

We thank Dr. Hodaka Kawahata of the National Institute of Advanced Industrial Science and Technology (AIST) for financing the IMAGES (WEPAMA) cruise. In 1984 when I. Koizumi started studying the hydrographic environments around the Tsugaru Strait, Drs. Akira Nishimura of the AIST and Yoshihiro Tanimura of the National Science Museum helped much in gripping the theme. We are grateful to Dr. John Barron of the U.S. Geological Survey and the unknown reviewer for their review and suggestions for improving this manuscript.

Appendix A. Supplementary data

Supplementary data associated with this article can be found, in the online version, at doi:10.1016/j.palaeo.2005.09.003.

References

Bard, E., 1998. Geochemical and geophysical implications of the radiocarbon calibration. Geo. Cos. Acta 62, 2025–2038.

Barron, J.A., Heusser, L., Herbert, T., Lyle, M., 2003. High-resolution climatic evolution of coastal northern California during the past 16,000 years. Paleoceaniography 18, doi:10.1029/2002PA000768.

Bond, G., Showers, W., Elliot, M., Evans, M., Lotti, R., Hadjas, I., Bonani, G., Johnson, S., 1999. The North Atlantic's 1–2 kyr climate rhythm: relation to Heinrich events, Dansgaard/Oeschger Cycles and the Little Ice Age. In: et al. (Eds.), Mechanisms of Global Climate Change at Millennial Time Scales, Am. Geophy. Union Monogr., vol. 112, pp. 385–394.

Fairbanks, R.G., 1990. The age and origin of the "Younger Dryas climate event" in Greenland ice cores. Paleoceaniography 5, 937–948.

Gorbarenko, S.A., Khusid, T.A., Basov, I.A., Oba, T., Southon, J.R., Koizumi, I., 2002. Glacial Holocene environment of the southeaster Okhotsk Sea: evidence from geochemical and palaeontological data. Palaeogeogr. Palaeoclimatol. Palaeoecol. 177, 237–263.

Hamblin, W.K., 1962. X-ray radiography in the study of structures in homogenous sediments. J. Sediment. Petrol. 32, 201–210.

Ikeda, M., Suzuki, F., Oba, T., 1999. A box model o glacial–interglacial variability in the Japan Sea. J. Oceanogr. Soc. Jpn 55, 483–492.

Ikehara, K., 2003. Late Quaternary seasonal sea-ice history of the northeastern Japan Sea. J. Oceanogr. Soc. Jpn 59, 585–593.

Ishiwatari, R., Yamada, K., Matsumoto, K., Houtatsu, M., Nakamura, H., 1999. Organic molecular and carbon isotopic records of the Japan Sea. Paleoceanography 14, 260–270.

Jian, Z., Li, B., Pflaumann, U., Wang, P., 1996. Late Holocene cooling event in the western Pacific. Sci. China, Ser. D: Earth Sci. 39, 543–550.

Kanaya, T., Koizumi, I., 1966. Interpretation of diatom thanatocoenoses from the North Pacific applied to a study of core V20-130 (studies of a deep-sea core V20-130, part IV). Sci. Rep. Tohoku Univ., Ser. 2 (37), 89–130.

Kawai, H., 1972. Hydrography of the Kuroshio extension. In: Stommel, H., Yoshida, K. (Eds.), Kuroshio—It's Physical Aspects. Univ. Tokyo Press, Tokyo, pp. 235–352.

Kennett, J.P., Ingram, B.L., 1995. A 20,000-year record of ocean circulatio and climate change fro the Santa Barbara basin. Nature 377, 510–514.

Koizumi, I., 1989. Holocene pulses of diatom growth in the warm Tsushima current in the Japan Sea. Diatom Res. 4, 55–68.

Koizumi, I., Shiga, K., Irino, T., Ikehara, M., 2003. Diatom record of the late Holocene in the Okhotsk Sea. Mar. Micropaleontol. 49, 139–156.

Koizumi, I., Irino, T., Oba, T., 2004. Paleoceanography off central Japa based on diatom flora during the latest Quaternary. Mar. Micropaleontol. 52, 293–365.

Li, B., Jian, Z., Wang, P., 1997. Pulleniatina obliquiloculata as a paleoceanographic indicator in the southern Okinawa Trough during the last 20,000 years. Mar. Micropaleontol. 32, 59–69.

Machida, H., Arai, F., 1992. Atlas of Tephras in and Around Japan. Univ. Tokyo Press, Tokyo. 276 pp. (in Japanese).

Martinson, D.G., Pisias, N.G., Hays, J.D., Imbrie, J., Moore Jr., T.C., Shackleton, N.J., 1987. Age dating and the orbital theory of the Ice Ages: development of a high-resolution 0 to 300, 000-year chronostratigraphy. Quat. Res. 1, 1–29.

Murayama, M., Yamane, M., Oka, S., Oba, T., Yamamoto, H., Yamauchi, M., 1999. Lithology of piston cores recovered fro the continental slope off the east coast of Honshu, Japan, during R/V "Mirai" MR97-04 cruise. JAMSTEC 39, 85–94 (in Japanese with English abstract).

Nakajima, T., Kikkawa, K., Ikehara, K., Katayama, H., Kikawa, E., Joshima, M., Seto, K., 1996. Marine sediments and late Quaternary stratigraphy in the southeastern part of the Japan Sea concerning the timing of dark-layer deposition. J. Geol Soc. Jpn 102, 125–138 (in Japanese with English abstract).

Narita, H., Sato, M., Tsunogai, S., Murayama, M., 2002. Biogenic opal indicating less productive northwester North Pacific during the glacial ages. Geophy. Res. Lett. 29, 22-1–22-4.

Oba, T., Kato, M., Kitazato, H., Koizumi, I., Omura, A., Sakai, T., Takayama, T., 1991. Paleoenvironmetal changes in the Japan Sea during the last 85,000 years. Paleoceanography 6, 499–518.

Oba, T., Murayama, M., Matsumoto, E., Nakamura, T., 1995. AMS-14C age of Japan Sea cores from the Oki Ridge. Quat. Res. 34, 289–296 (in Japanese with English abstract).

Oba, T., Murayama, M., Yamauchi, M., Yamane, M., Oka, S., Yamamoto, H., 1999. Oxygen isotopic ratio of Foraminiferal tests in marine sediment cores collected during "Mirai" MR97-04 cruise. JAMSTEC 39, 41–45 (in Japanese with English abstract).

Ohtani, K., Nishida, Y., 1990. Re-evaluation for the volume transport of the Tsushima warm current system. Abstracts of the Spring Convention in 1990 the Oceanogr. Soc. Japan, pp. 99–100 (in Japanese).

Onishi, M., Ohtani, K., 1997. Volume transport of the Tsushima Warm Current, west of Tsugaru Strait bifurcation area. J. Oceanogr. Soc. Jpn. 53, 27–34.

Sakaguchi, Y., 1982. Climatic variability during the Holocene epoch in Japan and its causes. Bull. Dep. Geogr. Univ. Tokyo 14, 1–27.

Sakaguchi, Y., 1983. Warm and cold stages in the past 7600 years in Japan and their global correlation especially on climatic impacts to the global sea level changes and the ancient Japanese history. Bull. Dep. Geogr Univ. Tokyo 15, 1–31.

Sancetta, C., 1982. Distribution of diatom species in surface sediments of the Bering and Okhotsk seas. Micropaleontology 28, 221–257.

Sancetta, C., Lyle, M., Heusser, L., Zahn, R., Bradbury, J.P., 1992. Late-glacial to Holocene change in winds, upwelling, and seasonal production of the northern California current system. Quat. Res. 38, 359–370.

Sheshukova-Poretskaya, V.S., 1964. New and rare diatoms in the Neogene of Sakhalin and Kamchatka. Akad. Nauk SSSR, Bot. Inst., Novitates Systematicae Plantaru non Vascularum 10, 69–72 (in Russian with English abstract).

Shiga, K., Koizumi, I., 2000. Latest Quaternary oceanographic changes in the Okhotsk Sea based on diatom records. Mar. Micropaleontol. 38, 91–117.

Shimada, C., Hasegawa, S., 1999. Late Quaternary paleoceanography in the northwestern Pacific margin reconstructed with a submarine core recovered off Sanriku: an approach using diatom fossil assemblage. Quat. Res. 38, 125–144 (in Japanese with English abstract).

Shimada, C., Murayama, M., Aoki, K., Nakamura, T., Hasegawa, S., 2000. Holocene paleoceanography in the SW part of the Sea of Okhotsk: a diato record. Quat. Res. 39, 439–449 (in Japanese with English abstract).

Shimada, C., Ikehara, K., Tanimura, Y., Hasegawa, S., 2004. Millennial-scale variability of Holocene hydrography in the southwestern Okhotsk Sea: diatom evidence. Holocene 14, 641–650.

Stuiver, M., Reimer, P.J., Bard, E., Beck, J.W., Burr, G.S., Hughen, K.A., Kromer, B., McCormac, G., van der Picht, J., Spurk, M., 1998. INTCAL98 radiocarbon age calibration, 24,000–0 cal BP. Radiocarbon 40, 1041–1083.

Tada, R., Koizumi, I., Cramp, A., Rahman, A., 1992. Correlation of dark and light layers, and the origin of their cyclicity in the Quaternary sediments from the Japan Sea. In: Pisciotto, K.A., Ingle Jr., J.C., von Breymann, M.T., et al. (Eds.), Proc. ODP, Sci. Results, vol. 127/128, Pt. 1. College Station, TX, pp. 577–601.

Tada, R., Irino, T., Koizumi, I., 1999. Land–ocean linkages over orbital and millennial timescales recorded in late Quaternary sediments of the Japan Sea. Paleoceanography 14, 236–247.

Takano, H., 1990. *Thalassionema nitzschioides* (Grunow) Grunow. In: Fukuyo, Y., Takano, H., Chihara, M., Matsuoka, K. (Eds.), Red Tide Organisms in Japan—An Illustrated Taxonomic Guide. Uchida Rokakuho, Tokyo, pp. 314–315.

Takei, T., Minoura, K., Tsukawaki, S., Nakamura, T., 2002. Intrusio of a branch of the Oyashi current into the Japan Sea during the Holocene. Paleoceanography 17, 11-1–11-10.

Yasuda, I., Okuda, K., Shimizu, Y., 1996. Distribution and modification of North Pacific Intermediate Water in the Kuroshio-Oyashio interfrontal zone. J. Phys. Oceanogr. 26, 448–465.

Yamamoto, H., 1999. Kuroshiowarm current changes during the past 20 thousand years in marine sediment cores collected during "Mirai" MR97-04 cruise. JAMSTEC 39, 95–109 (in Japanese with English abstract).